A Reduction Algorithm of Contact Problems for Core Seismic Analysis of Fast Breeder Reactors

Ryuta Imai[1] and Masatoshi Nakagawa[2]

Abstract: In order to evaluate seismic response of fast breeder reactors, finite element analysis for core vibration with contact/impact is performed so far. However a full model analysis of whole core vibration requires huge calculation times and memory sizes. In this research, we propose an acceleration method of reducing the number of degrees of freedom to be solved until converged for nonlinear contact problems. Furthermore we show a sufficient condition for the algorithm to work well and discuss its efficiency and a generalization of the algorithm. In particular we carry out the full model analysis to show that our method can decrease calculation time dramatically.

Keywords: reduction method, contact algorithm, core seismic analysis, Lagrange multiplier for constraints

1   Introduction

One of the primary requirements for nuclear power plants and facilities is to ensure safety and to prevent damage under strong external dynamic loading such as earthquakes. In a typical fast reactor, the core elements are, from the structural point of view, self-standing hexagonal beams supported by a core support structure and immersed in liquid sodium with very narrow spacing between adjacent ones at the pad levels. Thus, during a seismic event, their vibratory motion as a whole cluster may have a complicated and highly nonlinear nature due to contact/impact at pads between neighboring ones and dynamic fluid-structure interaction. The deflected core may have more reactivity due to core compaction and/or may hold back the control rod insertion. Therefore core seismic analysis is an important item to ensure fast reactor safety in an earthquake. General purpose FEM code such as ABAQUS requires huge calculation times and memory sizes for analyzing nonlinear contact problems. In this paper we propose a new method to facilitate the time consuming

[1] Mizuho Information & Research Institute, Inc., Japan
[2] Toyo University, Japan

nonlinear time history calculation by reducing the number of degrees of freedom to be solved until converged at each time step of nonlinear contact problems. Furthermore, we show a sufficient condition for the algorithm to work well and discuss its efficiency and a generalization of the algorithm. Especially we do the full model analysis to show that our method can decrease calculation time dramatically.

The IAEA Working Group on LMFBR has approved the Coordinated Research Programme (CRP) on Intercomparison of LMFBR Seismic Analysis Codes after the year at its meeting in April 1990. The results have been published in the three reports [IAEA (1993), IAEA (1994), IAEA (1995)]. Nine codes from five countries participated to the CRP. In the nine codes, only one code named SALCON [Kobayashi, T. (1995)] has the special features like our proposed new method to facilitate the time consuming nonlinear time history calculation. SALCON employs the Guyan Reduction for reducing dynamically unimportant freedoms. The Guyan Reduction is made based on static approximation, hence the dynamic calculation accuracy seems to have some errors. Another finite element code named ARKAS [Nakagawa, M. (1986)] was used for prediction of static distortion of FBR cores. A substructure method is employed in ARKAS. However, dynamic response of core vibration is not dealt with in ARKAS.

2   Contact algorithm

In the core of an FBR, at most a few kinds of core elements are located along concentric circle (hexagon) and their total amount attains over 700 components. As in Fig.1, neighboring elements may contact/impact through their load pads and show strongly nonlinear behavior caused by their contact/impact. In what follows, we find some features of core seismic analysis and propose a contact algorithm adapted to these features.

2.1   Features and formulations

It is of worth to remark that the core elements are independent beam-like structures whenever these do not contact/impact.(See Fig.2.) In our algorithm we will use positively the following features of core seismic analysis.

(a) Only contact/impact through load pads causes nonlinearity of deformation behaviors of the core.

(b) The whole core consists of independent assemblies whenever they do not contact/impact.

With numbering nodes of FEM, we can make a matrix, which appears in a procedure in FEM, to be direct sums of a small matrix which corresponds to an as-
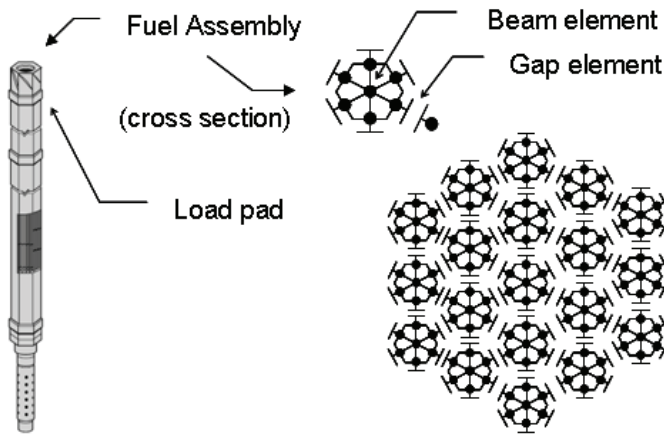
Figure 1: Fuel assembly (left) and core configuration of cross section (right)
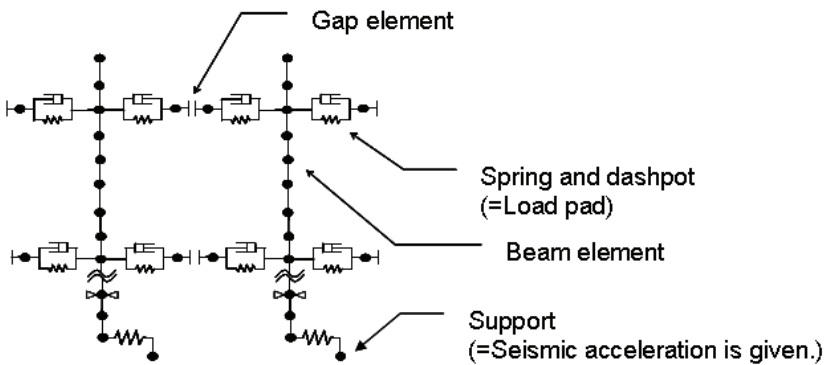

Figure 2: FEM model of core seismic analysis

sembly in the core. Contact/impact is treated by introducing the Lagrange multiplier method for constraints of gap elements. By ordering degrees of freedom of Lagrange multipliers to separator degrees of freedom, we may let the matrix be bordered block diagonal. Then, the matrix shape is as follows:

(a') The whole shape is bordered block diagonal (with separators corresponding to constraints between pads).

(b') Block diagonal parts are direct sums of a small matrix corresponding to each assembly.

Such technique, which divides a matrix into the shape above, is well-known. The essence of our algorithm is how we apply the technique to the time marching non-linear problems in order to reduce the number of degrees of freedom which must be operated within the time step loop. Especially the key point of our algorithm is that we can deal with time-variable number of separator degrees of freedom.

Now some features about border parts and block diagonal parts should be mentioned as follows:

(a") Border parts may change from time to time.

(b") Block diagonal parts do not change. (They are independent with respect to deformation and contact/impact status.)

We will show the details of these features (a'), (b') or (a"), (b") in the sequel. Now, we derive space-wise discretized equations of core seismic analysis with contact/impact. We let kinetic energy and potential energy be

$$K = \frac{1}{2}\{\dot{U}\}^T[M]\{\dot{U}\},\tag{1}$$

$$V = -\{U\}^T\{F\} + \int_V W\,dV,\tag{2}$$

respectively, where $\{U\}$ is a displacement vector, $\{F\}$ is an external force vector, $[M]$ is a mass matrix, $W = \int_0^\varepsilon \sigma_{ij}d\varepsilon_{ij}$ is strain energy density, σ and ε are stress and strain tensors. For any variation $\{\delta U\}$ of displacement, kinetic energy variation and potential energy variation are

$$\delta K = \lim_{h\to 0}\frac{K(U + h\delta U) - K(U)}{h} = \{\delta \dot{U}\}^T[M]\{\dot{U}\},\tag{3}$$

$$\delta V = \lim_{h\to 0}\frac{V(U + h\delta U) - V(U)}{h} = -\{\delta U\}^T\{F\} + \int_V \{\delta \varepsilon\}^T\{\sigma\}\,dV,\tag{4}$$

where we used $\delta W = \frac{\partial W}{\partial \varepsilon_{ij}}\delta \varepsilon_{ij} = \sigma_{ij}\delta \varepsilon_{ij} = \{\delta \varepsilon\}^T\{\sigma\}$.

We define the augmented Lagrangian L and the action integral I on a time interval (s,t) as

$$L(U,\Lambda) = K - V - \{G\}^T\{\Lambda\},\tag{5}$$

$$I = \int_s^t L\,dt,\tag{6}$$

where $\{G\} = 0$ is a constraint condition of gap elements and $\{\Lambda\}$ is a Lagrange multiplier conjugated to the constraint. If the variation $\{\delta U\}$ of displacement satisfies a boundary condition $\delta U(s) = \delta U(t) = 0$, the stationarity of I and equations (3), (4) yield that

$$
\begin{aligned}
0 &= \delta I \\
&= \int_s^t \delta L \, dt \\
&= \int_s^t \{\delta U\}^T \left(-[M]\{\ddot{U}\} + \{F\} - \int_V [B]^T \{\sigma\} \, dV - \left(\frac{\partial G}{\partial U}\right)^T \{\Lambda\} \right) dt \\
&\quad - \int_s^t \{\delta \Lambda\}^T \{G\} \, dt,
\end{aligned}
\tag{7}
$$

where $[B]$ is an operator which corresponds nodal displacement $\{U\}$ to strain $\{\varepsilon\}$. From this equation (7), we can get

$$
[M]\{\ddot{U}\} + \int_V [B]^T \{\sigma\} \, dV + \left(\frac{\partial G}{\partial U}\right)^T \{\Lambda\} = \{F\},
\tag{8}
$$

$$
\{G\} = 0,
\tag{9}
$$

because variations $\{\delta U\}$ and $\{\delta \Lambda\}$ are arbitrary. Assuming the energy dispersion by velocity proportional damping, a matrix $[C]$ is added into equation (8) to derive the equation of motion

$$
[M]\{\ddot{U}\} + [C]\{\dot{U}\} + \int_V [B]^T \{\sigma\} \, dV + \left(\frac{\partial G}{\partial U}\right)^T \{\Lambda\} = \{F\}.
\tag{10}
$$

Next we explore time integration scheme of the basic equation (10). We linearize these equations (9) and (10) with the Newton-Raphson method to have

$$
\begin{pmatrix} [M] & 0 \\ 0 & 0 \end{pmatrix} \begin{pmatrix} \{d\ddot{U}\} \\ \{d\ddot{\Lambda}\} \end{pmatrix} + \begin{pmatrix} [C] & 0 \\ 0 & 0 \end{pmatrix} \begin{pmatrix} \{d\dot{U}\} \\ \{d\dot{\Lambda}\} \end{pmatrix} + \begin{pmatrix} [K] & [H]^T \\ [H] & 0 \end{pmatrix} \begin{pmatrix} \{dU\} \\ \{d\Lambda\} \end{pmatrix} = \begin{pmatrix} \{R_1\} \\ \{R_2\} \end{pmatrix},
\tag{11}
$$

where $[H] = [dG/dU]$ is a Jacobian of constraint, $[K]$ is a tangent stiffness matrix and $\{R_1\}$ and $\{R_2\}$ are residuals. The time integration is performed by the Newmark-beta method [Geradin, M. and Cardona, A. (2001)] or the Generalized-alpha method, in which velocity is adopted as a primal unknown variable. That is, displacement $\{U^{n+1}\}$ and acceleration $\{A^{n+1}\} = \{\ddot{U}^{n+1}\}$ at instantaneous time

t^{n+1} are assumed to be represented by the known values $\{U^n\}$, $\{V^n\} = \{\dot{U}^n\}$ and $\{A^n\}$ at time t^n and the unknown value $\{V^{n+1}\}$ at time t^{n+1}.

$$\{U^{n+1,(i)}\} = \frac{\beta \Delta t}{\gamma} \left(\{V^{n+1,(i)}\} - \{V^n\}\right) + \{U^n\} + \Delta t \{V^n\} + \left(\frac{1}{2} - \frac{\beta}{\gamma}\right) \Delta t^2 \{A^n\},$$

$$\{A^{n+1,(i)}\} = \frac{1}{\gamma \Delta t} \left(\{V^{n+1,(i)}\} - \{V^n\}\right) + \left(1 - \frac{1}{\gamma}\right)\{A^n\}, \tag{12}$$

where β and γ are parameters, Δt is a time step size and superscripts n and (i) indicate time step number and iteration number respectively. Then, displacement and acceleration corrections $\{dU^{n+1,(i+1)}\}$ and $\{dA^{n+1,(i+1)}\}$ are expressed by velocity correction $\{dV^{n+1,(i+1)}\} = \{V^{n+1,(i+1)}\} - \{V^{n+1,(i)}\}$.

$$\{dU^{n+1,(i+1)}\} = \frac{\beta \Delta t}{\gamma} \{dV^{n+1,(i+1)}\}. \tag{13}$$

$$\{dA^{n+1,(i+1)}\} = \frac{1}{\gamma \Delta t} \{dV^{n+1,(i+1)}\}. \tag{14}$$

Substituting equations (13) and (14) into (11), we can conclude that

$$\begin{pmatrix} \frac{1}{\gamma \Delta t}[M] + [C] + \frac{\beta \Delta t}{\gamma}[K] & [H]^T \\ [H] & 0 \end{pmatrix} \begin{pmatrix} \{dV^{n+1,(i+1)}\} \\ \{d\Lambda^{n+1,(i+1)}\} \end{pmatrix} = \begin{pmatrix} \{R_1^{n+1,(i)}\} \\ \{R_2^{n+1,(i)}\} \end{pmatrix}. \tag{15}$$

2.2   Reduction algorithm

Equation (15) shows that the matrix has diagonal parts corresponding to core elements and border parts corresponding to constraint of contact/impact. Especially diagonal parts may assume to be direct sums of a small matrix for an assembly because whole-core consists of independent assemblies whenever they do not contact/impact. Moreover diagonal parts may assume to be invariant with respect to time because their structures do not change. In what follows we assume that the numbering of nodal points in the FEM model is sequential in every assembly. Then mass matrix, damping matrix and stiffness matrix are represented by

$$[M] = \begin{pmatrix} [M_{(1)}] & 0 & 0 \\ 0 & \ddots & 0 \\ 0 & 0 & [M_{(N)}] \end{pmatrix}, \tag{16}$$

$$[C] = \begin{pmatrix} [C_{(1)}] & 0 & 0 \\ 0 & \ddots & 0 \\ 0 & 0 & [C_{(N)}] \end{pmatrix}, \tag{17}$$

$$[K] = \begin{pmatrix} [K_{(1)}] & 0 & 0 \\ 0 & \ddots & 0 \\ 0 & 0 & [K_{(N)}] \end{pmatrix}, \tag{18}$$

where $[M_{(i)}]$, $[C_{(i)}]$ and $[K_{(i)}]$ are mass matrix, damping matrix and stiffness matrix of the i-th assembly respectively. If the shape and material (and boundary condition) of the i-th assembly and of the j-th assembly coincide with each other, we have that $[M_{(i)}] = [M_{(j)}]$, $[C_{(i)}] = [C_{(j)}]$ and $[K_{(i)}] = [K_{(j)}]$. So we may store only at most a few kinds of small matrices for different assemblies.

In the case that a contact is modeled by a gap element between two adjacent assemblies, we consider the gap element to consist of the p-th node in the i-th one assembly and the q-th node in the j-th another assembly. Let us denote their nodal displacements as $\{U^p\}$, $\{U^q\}$ and nodal initial positions as $\{X^p\}$, $\{X^q\}$. Then we conclude this gap element closes if the relative displacement along the gap direction reaches the initial gap distance. This condition for closed gap element is satisfied by the following constraint.

$$\{U^{pq}\} \cdot \{X^{pq}\} + d_0 = 0, \tag{19}$$

where d_0 is an initial gap distance, $\{U^{pq}\} = \{U^q\} - \{U^p\}$ is a relative displacement, $\{X^{pq}\} = \frac{\{X^q\} - \{X^p\}}{\|\{X^q\} - \{X^p\}\|}$ is a gap direction and $\{U^{pq}\} \cdot \{X^{pq}\}$ is the inner product. Using velocity variables we rewrite the constraint (19) to yield

$$\{V^{pq}\} \cdot \{X^{pq}\} = 0, \tag{20}$$

where $\{V^{pq}\} = \{V^q\} - \{V^p\}$ is a relative velocity. The Jacobian of this constraint (19) or (20) is

$$\{h_{(i)}\} = \left(0, \cdots, 0, \{X^{pq}\}^T, 0, \cdots, 0\right). \tag{21}$$

In equation (21), nonzero components $\{X^{pq}\}$ are located according to the numbering of the p-th node in the i-th assembly. Substituting representations (16), (17) and (18) of diagonal parts and Jacobian (21) of constraints into equation (15), we

finally have

$$
\begin{pmatrix}
[A_{(1)}] & 0 & 0 & 0 & 0 & 0 & 0 & 0 \\
0 & \ddots & 0 & 0 & 0 & 0 & 0 & 0 \\
0 & 0 & [A_{(i)}] & 0 & 0 & 0 & 0 & +\{h_{(i)}\}^T \\
0 & 0 & 0 & \ddots & 0 & 0 & 0 & 0 \\
0 & 0 & 0 & 0 & [A_{(j)}] & 0 & 0 & -\{h_{(j)}\}^T \\
0 & 0 & 0 & 0 & 0 & \ddots & 0 & 0 \\
0 & 0 & 0 & 0 & 0 & 0 & [A_{(N)}] & 0 \\
0 & 0 & +\{h_{(i)}\} & 0 & -\{h_{(j)}\} & 0 & 0 & 0
\end{pmatrix}
\begin{pmatrix}
\{dV_{(1)}\} \\ \vdots \\ \{dV_{(i)}\} \\ \vdots \\ \{dV_{(j)}\} \\ \vdots \\ \{dV_{(N)}\} \\ \{d\Lambda\}
\end{pmatrix}
$$

$$
=
\begin{pmatrix}
\{R_{(1)}\} \\ \vdots \\ \{R_{(i)}\} \\ \vdots \\ \{R_{(j)}\} \\ \vdots \\ \{R_{(N)}\} \\ \{R_{(\lambda)}\}
\end{pmatrix}, \quad (22)
$$

where subscript indicates the assembly number and

$$
[A_{(n)}] = \frac{1}{\gamma \Delta t}[M_{(n)}] + [C_{(n)}] + \frac{\beta \Delta t}{\gamma}[K_{(n)}]. \tag{23}
$$

If many gap elements close, we may arrange the Jacobian $\{h_{(i)}\}$ for all closed gap elements. From now on, we denote the matrix of the left hand side of equation (22) for simplicity as

$$
A =
\begin{pmatrix}
A_{(1)} & 0 & 0 & H_{(1)}^T \\
0 & \ddots & 0 & \vdots \\
0 & 0 & A_{(N)} & H_{(N)}^T \\
H_{(1)} & \cdots & H_{(N)} & 0
\end{pmatrix}. \tag{24}
$$

Before we explore the reduction method, two properties of the matrix A should be mentioned here. Suppose that N is the number of assemblies and M is the number of closed gap elements. Then we consider the following two properties.

(p1) $A_{(i)}$ is positive definite symmetry.

(p2) $rank\left(H_{(1)} \quad \cdots \quad H_{(N)}\right) = M.$

In general, mass matrix and stiffness matrix are positive definite symmetry respectively. So the property (p1) is satisfied because parameters β and γ are positive. The property (p2) is only hypothesis, but we may assume this hypothesis is often satisfied in practice. This is because elements such as spring and dashpot are inserted around gaps. (See section 3.1 in detail.) Now, we claim a statement:

Statement 1. *Suppose a matrix A satisfies two properties (p1) and (p2), then A can be decomposed as follows.*

$$A = LU = \begin{pmatrix} L_{(1)} & 0 & 0 & 0 \\ 0 & \ddots & 0 & 0 \\ 0 & 0 & L_{(N)} & \\ l_{(1)} & \cdots & l_{(N)} & L' \end{pmatrix} \begin{pmatrix} L_{(1)}^T & & & l_{(1)}^T \\ & \ddots & & \vdots \\ & & L_{(N)}^T & l_{(N)}^T \\ & & & U' \end{pmatrix}, \tag{25}$$

where $L_{(i)}$ and L' are lower triangle and U' is upper triangle.

In fact, by comparing the right hand side of equation (25) with the right hand side of equation (24), we have

$$A_{(i)} = L_{(i)}L_{(i)}^T \quad (i = 1,...,N), \tag{26}$$

$$H_{(i)}^T = L_{(i)}l_{(i)}^T \quad (i = 1,...,N), \tag{27}$$

$$0 = \sum_{i=1}^{N} l_{(i)}l_{(i)}^T + L'U'. \tag{28}$$

Because of the property (p1) each $A_{(i)}$ can be Cholesky decomposed to yield equation (26). We can get each $l_{(i)}$ by forward substitutions of equation (27). The property (p2) leads us to the fact that $\sum_{i=1}^{N} l_{(i)}l_{(i)}^T = \sum_{i=1}^{N} H_{(i)}A_{(i)}^{-1}H_{(i)}^T$ is positive definite symmetry. Therefore there is a lower triangle matrix L' such that $L'(L')^T = \sum_{i=1}^{N} l_{(i)}l_{(i)}^T$. We may let $U' = -(L')^T$ to conclude the statement.

In our reduction algorithm it is important that every diagonal part $A_{(i)}$ of the total matrix A is invariant with respect to time because $[M_{(i)}]$, $[C_{(i)}]$ and $[K_{(i)}]$ do not change. In other words only border parts $H_{(i)}$ may change from time to time. Using this fact and the proof of statement 1, we find that the diagonal parts $L_{(i)}$ is time-independent and border parts $l_{(i)}$, diagonal parts L' and U' may change from time to time according to contact status. We should remark that the sizes of $l_{(i)}$, L' and U' may also change from time to time.(See Tab.1.)

Table 1: Time dependency of matrix components

	time-independent	time-dependent
Before decomp.	$A_{(i)}$	$H_{(i)}$
After decomp.	$L_{(i)}$	$l_{(i)}, \quad L', \quad U'$
After decomp. (modified)	$L_{(i)}, \quad \tilde{l}_{(i)}, \tilde{H}_{(i)}$	$L', \quad U'$

Since $A_{(i)}$ and $L_{(i)}$ are time-independent, the procedure of the Cholesky decomposition $A_{(i)} = L_{(i)}L_{(i)}^T$ can be done only once outside the loop of time marching. On the other hand, we must do the procedures of the forward substitution $H_{(i)}^T = L_{(i)}l_{(i)}^T$ and the Cholesky decomposition $L'(L')^T = \sum_{i=1}^{N} l_{(i)}l_{(i)}^T$ within the loop since $H_{(i)}$, $l_{(i)}$, L' and U' are time-dependent. Of course, we need to do nothing for time-dependent components if any contact/impact does not occur. The number of degrees of freedom for time-dependent components coincides with the number of active constraints of contact/impact. So the number of time-dependent components is relatively small compared with the total number of time-independent components. That is to say, by extracting time-dependent components from the total system matrix, we can reduce the number of degrees of freedom which must be operated within the time step loop. Moreover we can consider time-independent components $\tilde{l}_{(i)}$ as substitutes for time-dependent components $l_{(i)}$ in this problem. This is because we suppose that all gap elements contact/impact to get constant border parts $\tilde{H}_{(i)}$ and we then have constant components $\tilde{l}_{(i)}$ such that $\tilde{H}_{(i)}^T = L_{(i)}\tilde{l}_{(i)}^T$. We can easily find a Boolean matrix $N_{(i)}$ such that $l_{(i)} = N_{(i)}\tilde{l}_{(i)}$. It is remarked that multiplying the Boolean matrix $N_{(i)}$ means adaptive selection of the actual closed gap element. Then we may do only the Cholesky decomposition $L'(L')^T = \sum_{i=1}^{N} N_{(i)}\tilde{l}_{(i)}\tilde{l}_{(i)}^T N_{(i)}^T$ within the time step loop. We show a schematic procedures for the matrix operations above in Fig.3.

Next we explore concrete operations within the time step loop. Suppose that the Cholesky decomposition (26) is already done outside the loop. In order to solve an equation $Ax = b$, we may let

$$y = \begin{pmatrix} y_{(1)} \\ \vdots \\ y_{(N)} \\ y' \end{pmatrix} = Ux \tag{29}$$
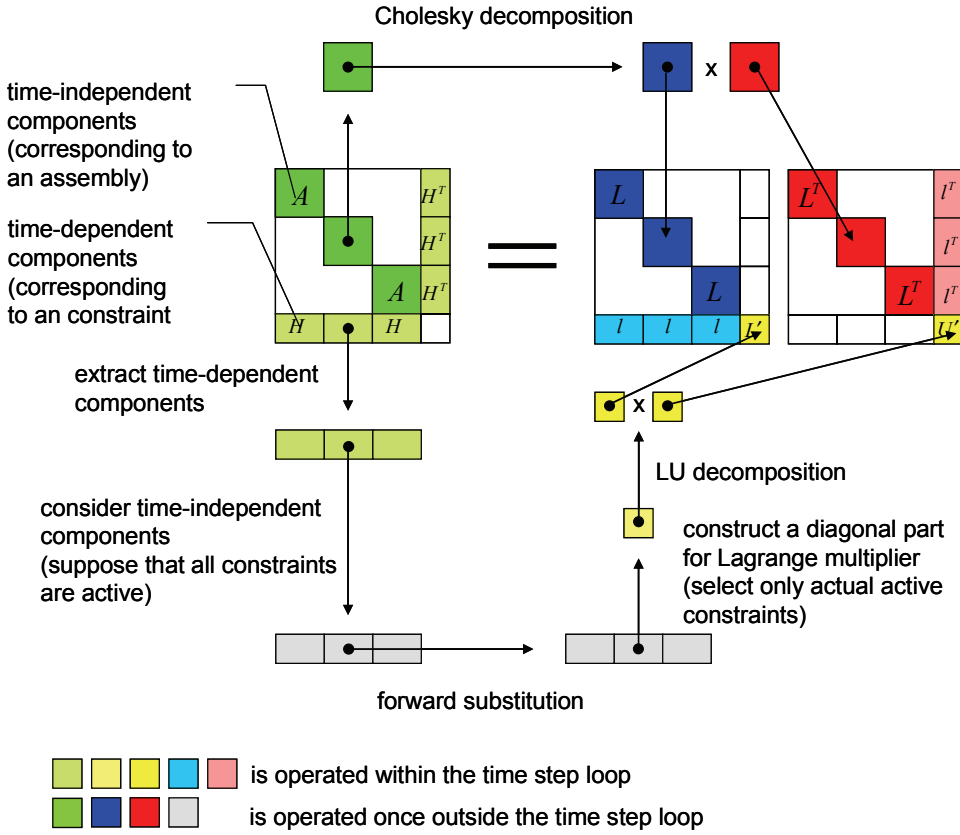
Figure 3: Schematic procedures of a reduction method for matrix operations

to consider the following equation below.

$$
Ly = \begin{pmatrix} b_{(1)} \\ \vdots \\ b_{(N)} \\ b' \end{pmatrix}. \tag{30}
$$

Here it is noted that the border part $l_{(i)}$ and the LU-decomposition (28) should be operated within the loop. Since each block diagonal part $L_{(i)}$ of L is lower triangle, a forward substitution yields a solution $y_{(i)}$ of equation (30) for any (i). Using such solution $y_{(i)}$, we have an equation

$$
L'y' = b' - \sum_{i=1}^{N} l_{(i)} y_{(i)}. \tag{31}
$$

The right hand side of (31) is now already known and L' is also lower triangle. So the same way leads us to a solution y' of equation (31). By gathering each solution $y_{(i)}$ and y', we finally get the solution of equation (30). Then we must solve the equation $Ux = y$. Since U' is upper triangle, we can solve the equation $U'x' = y'$ by a backward substitution. Using such solution x', the following equations are considered for each block part.

$$L_{(i)}^T x_{(i)} = b_{(i)} - u_{(i)}^T y' \quad (i = 1,...,N). \tag{32}$$

Since $L_{(i)}^T$ is upper triangle, we can get a solution $x_{(i)}$ of equation (32). Each solution $x_{(i)}$ and x' yield the solution of the equation $Ax = b$. As is mentioned above, we may use time-independent components $\tilde{l}_{(i)}$, which is made once outside the loop, and we can operate only the Cholesky decomposition $L'(L')^T = \sum_{i=1}^N N_{(i)} \tilde{l}_{(i)} \tilde{l}_{(i)}^T N_{(i)}^T$ within the loop. In Fig.4, we show the flow chart of the procedures.

3 Discussion

Now we show a sufficient condition for the algorithm to work well and discuss its efficiency of the proposed reduction method. We also mention a generalization of the method.

3.1 A sufficient condition

As is mentioned in section 2.2, the proposed algorithm can not be necessarily accomplished successfully if the border parts do not have full rank. (See the property (p2) in section 2.2.) In what situation do we satisfy the condition? Here we give an answer to the question.

Statement 2. *Suppose any node is included in at most one gap element, then the Jacobian of constraints of contact/impact has full rank.*

In other words, this proposed algorithm can be accomplished successfully whenever none of all nodes are shared by more than one gap element. We show a rough sketch of the proof of this statement. Each row of the Jacobian H of constraints of contact/impact corresponds to a constraint condition of a gap element. For example, we suppose that two nodes of this closed gap element consist of the p-th node and the q-th node. The constraint condition of this situation is as follows.

$$(V^q - V^p) \cdot N = 0, \tag{33}$$

where $V^p = (V_1^p, V_2^p, V_3^p)$ and $V^q = (V_1^q, V_2^q, V_3^q)$ are the velocity vectors of the p-th node and the q-th node respectively and $N = (N_1, N_2, N_3)$ is the unit vector along
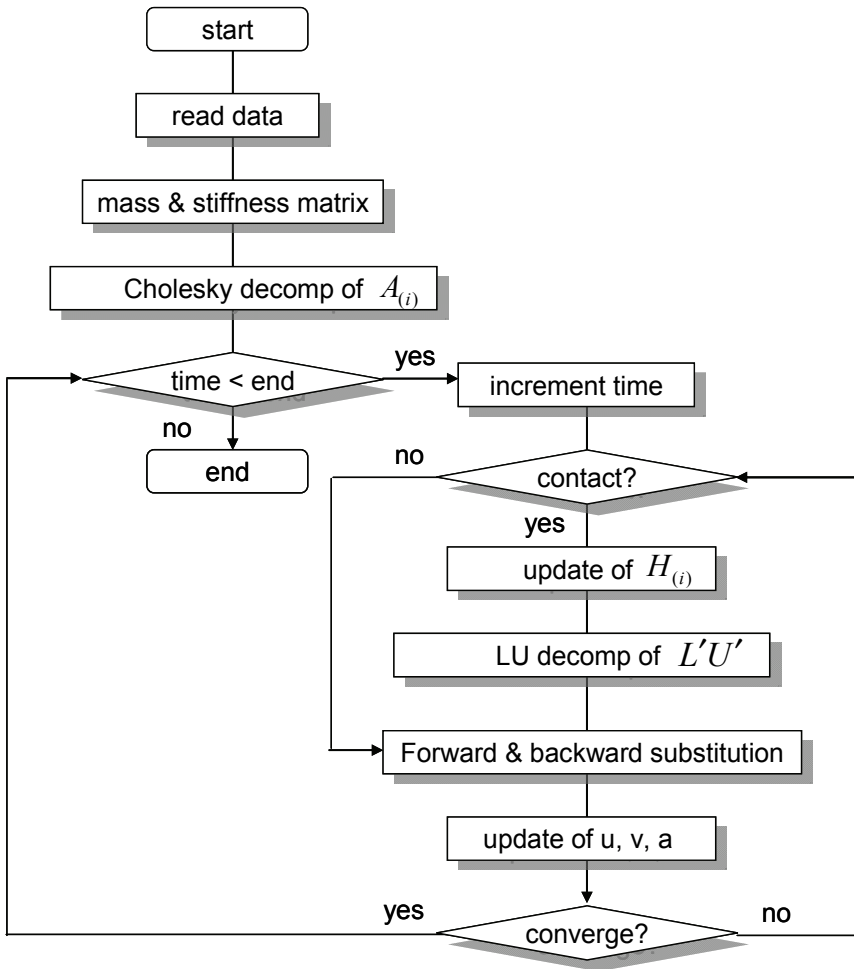
Figure 4: Flow chart of the procedure

the axial direction of the gap element. Writing this condition by components, we have

$$V_i^q N_i - V_i^p N_i = 0. \tag{34}$$

This expression means that the row vector of the Jacobian H corresponding to the constraint condition of the gap element is written as follows.

$$h = (0, ..., 0, N_1, N_2, N_3, 0, ..., 0, -N_1, -N_2, -N_3, 0, ..., 0). \tag{35}$$

Of course, positions of the non zero components depend on the numbering of these

nodes. If there are two row vectors h_1 and h_2 of the Jacobian H such that a position of non zero components of the two vectors coincides with each other, at least one node of the corresponding gap elements is shared by the gap elements. This is a contradiction. Thus we conclude that any two row vectors of the Jacobian H have a different position of non zero components from each other. This shows that row vectors of the Jacobian H are linearly independent and they have full rank.

In most practical cases of the core seismic analysis, we impose spring and dashpot elements and introduce a damping effect in order to improve the convergence of contact/impact problems. In such cases, even if some nodes are shared by one gap element, none of the nodes are shared by more than one gap element. The statement 2 above guarantees that the Jacobian H of the constraint condition has full rank.

3.2 Efficiency

The features of the algorithm proposed in this paper are the following:

(A) The only LU-decomposition of equation (28) is done within the time step loop and the size of this matrix coincides with the time-variable number of closed gap elements simultaneously in a step.

(B) We need not to store all block diagonal parts of the total matrix. (We may store only at most a few kinds of matrices for different kinds of assemblies.)

These two features correspond to the features of the core seismic analysis mentioned in section 2.1. From the feature (A), we can reduce the number of degrees of freedom which are LU-decomposed within the time step loop and save the calculation time if the number of closed gap elements simultaneously in a step is small. For instance, we assume that the total number of the core elements is N and the number of nodes in an assembly is n. Then we can approximately estimate the number N_{GAP} of all gap elements by $N_{GAP} = 3N$ when the assemblies are located along concentric circle (hexagon). (Considering the triangle consisting of three assemblies located adjacently each other, three vertexes are shared by six neighboring triangles. By contrast, three edges are shared by two neighboring triangles.) If we assume that the number N_{GAP_ACTIVE} of closed gap elements simultaneously in a step is proportional to the diameter of the whole core, we have $N_{GAP\_ACTIVE} \approx \sqrt{N}$. Hence we can estimate the computational complexity A needed by the LU-decomposition of a small matrix derived from equation (28) as

$$A \approx (N_{GAP\_ACTIVE})^3 \approx N^{3/2} \tag{36}$$

because it is a dense matrix. On the other hand, the total number N_{DOF} of degrees of freedom except for the Lagrange multipliers is $N_{DOF} = 6nN$. (We model the

core elements by the beam element and assume the number of degrees of freedom in a node is six.) If we assume that a band width W_{BAND} of the total matrix is proportional to both of the diameter of the whole core and the number of nodes in an assembly, we have $W_{BAND} \approx n\sqrt{N}$. Thus the computational complexity A' needed by the LU-decomposition of the total matrix is estimated as

$$A' \approx (N_{DOF} + N_{GAP\_ACTIVE})^2 \cdot W_{BAND} \approx \{6nN + \sqrt{N}\}^2 \cdot n\sqrt{N} \approx n^3 N^{5/2} \qquad (37)$$

since the total matrix is sparse. Comparing A with A', we find that the computational complexity of the proposed method is reduced to be about $\frac{A}{A'} \approx \frac{1}{n^3 N}$ times of the usual method. Next we estimate the memory size B' needed for all matrix $A_{(i)}$ by

$$B' \approx (6n)^2 N \approx n^2 N. \qquad (38)$$

On the other hand, the feature (A) above shows that the memory size B needed for the proposed method is

$$B \approx (6n)^2 m \approx n^2 m. \qquad (39)$$

Then we compare B with B' to conclude that the memory size of the proposed method is reduced to be about $\frac{B}{B'} \approx \frac{m}{N}$ times of the usual method. From these considerations above, it is found that the more the number of assemblies and the number of node in an assembly increase, the more effective this technique becomes.

3.3 A generalization

The reduction method proposed in this paper is applicable to more generalized problems. Here we give a guide for applying the method to generalized problems. Consider the following two properties of the problem.

(pA) The components, which can change from time to time, are restricted locally in the whole system.

(pB) Extracting the changeable components from the whole system, the resultants consist of independent and invariant small components.

For instance, we recall an electric circuit in which the structure of the circuit may change by switching. The changeable components of this circuit are only small parts around the switch and other parts except for the switch are invariant. Such an electric circuit satisfies the two properties above. As another instance, we recall a device with some designed constraints such as contact or motion. Contact parts

or motion parts of the device are specified in advance and the structure of resulting parts after eliminating such changeable parts does not change. An FBR in the core seismic analysis corresponds to that device. Especially the features (a) and (b) of the core seismic analysis mentioned in section 2.1 correspond to the properties (pA) and (pB) of the generalized problem respectively. A whole system satisfying the properties (pA) and (pB) is abstractly represented as follow:

$$A(t)x(t) = b(t), \tag{40}$$

where $A(t)$ is the property of the system at time instance t, $x(t)$ is the status of the system and $b(t)$ is the input of the system from external actions. Then we divide the system into the independent subsystem and the time dependent small subsystem via the properties (pA) and (pB). We denote the status $x(t)$ of the system as $x(t) = (x'(t), x''(t))$ according to the system division. Using this division, the system matrix $A(t)$ can be expressed as

$$A(t) = \begin{pmatrix} A_0 & C(t) \\ B(t) & D(t) \end{pmatrix}. \tag{41}$$

Now, assume that the component A_0 corresponding to the time invariant property in the whole system is positive definite. Then a time invariant LU-decomposition $A_0 = L_0 U_0$ can be done. Let matrix $L'(t)$ and $U'(t)$ to be

$$L'(t) = B(t)U_0^{-1},$$

$$U'(t) = L_0^{-1}C(t), \tag{42}$$

respectively with constant triangle matrix L_0 and U_0. If $D(t) - L'(t)U'(t) = D(t) - B(t)A_0^{-1}C(t)$ can be LU-decomposed and there are lower triangle matrix $L''(t)$ and upper triangle matrix $U''(t)$ such that

$$D(t) - L'(t)U'(t) = L''(t)U''(t), \tag{43}$$

the following holds.

$$A(t) = \begin{pmatrix} A_0 & C(t) \\ B(t) & D(t) \end{pmatrix} = \begin{pmatrix} L_0 & 0 \\ L'(t) & L''(t) \end{pmatrix} \begin{pmatrix} U_0 & U'(t) \\ 0 & U''(t) \end{pmatrix}. \tag{44}$$

Therefore we may do the LU-decomposition $A_0 = L_0 U_0$ only once outside the time step loop. On the other hand, the forward/backward substitution for L_0, U_0 and the LU-decomposition $D(t) - L'(t)U'(t) = L''(t)U''(t)$ must be done within the time step loop. In the case that the components, which may change from time to time,

are relatively small in the whole system, this generalized algorithm contributes to the reduction of computational complexity within the time step loop. Using this generalized algorithm we can implement the core seismic analysis program with penalty method too. As is easily shown, the formulation of the penalty method makes a matrix in FEM to have no border parts. Instead the parts $B(t)$, $C(t)$ and $D(t)$ are renewed according to the contact status. At this time it is necessary to note that A_0 does not correspond to the assemblies themselves and that A_0 corresponds to the remainders from which the load pads are removed instead. We also mention that the matrix components for load pads are included in $B(t)$, $C(t)$ and $D(t)$ even if they do not contact. In the formulation with the Lagrange multiplier method, however, A_0 corresponds to the assemblies themselves and $B(t)$, $C(t)$ and $D(t)$ are simply zeros whenever they do not contact. Moreover, as mentioned in section 2.2, we can use constant matrices $\bar{B}$ and $\bar{C}$ instead of $B(t)$ and $C(t)$ to make forward/backward substitutions

$$\bar{L}' = \bar{B}U_0^{-1}, \tag{45}$$

$$\bar{U}' = L_0^{-1}\bar{C}. \tag{46}$$

$\bar{B}$ and $\bar{C}$ are the matrix which correspond to the status that the all gap elements contact/impact. In fact we make Boolean matrices $N_B(t)$ and $N_C(t)$, which components represent the position of contact/impact gap element (0 represents non contact/impact and 1 represents contact/impact), to have

$$B(t) = N_B(t)\bar{B}, \tag{47}$$

$$C(t) = \bar{C}N_C(t). \tag{48}$$

Thus the forward/backward substitutions of equations (45), (46) may also be done once outside the time step loop and the only LU-decomposition $D(t) - L'(t)U'(t) = L''(t)U''(t)$ can be done within the time step loop. That is to say, we can generalize our algorithm to apply it for the problems satisfying the two properties above.

4   Core seismic analysis

4.1   Verification analysis

As a verification analysis we give a test problem of three assemblies with gap elements to show that our proposed algorithm works reasonably well. In this problem we give a step load to the left assembly. The left assembly contacts/impacts with the center assembly and the center assembly starts to vibrate. Then the center assembly contacts/impacts with the right assembly and the right assembly starts to vibrate. The applied model is as follows in Fig.5.

Table 2: Material properties of test assemblies

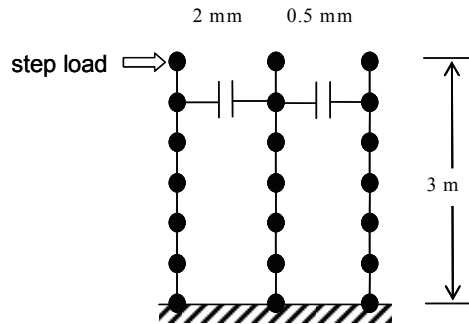|	density [kg/m^3]	Young's modulus [Pa]	Poisson ratio [-]	cross section [m^2]	second moment of area [m^4]
Left	1.0e4	2.0e11	0.3	1.0e-2	2.0e-6
Center	0.5e4	2.0e11	0.3	1.0e-2	2.0e-6
Right	1.0e4	2.0e11	0.3	1.0e-2	2.0e-6

Figure 5: FEM model of a test problem
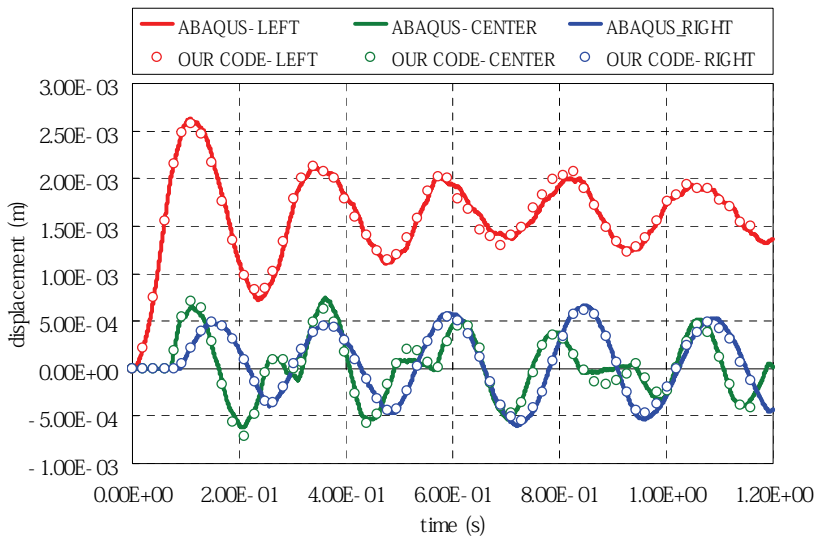
Figure 6: Time history of the left, center and right assemblies

We set material properties of three assemblies as as in Tab.2.

Fig.6 below shows time historical data of displacements of the left, center and right assemblies respectively. It is found that each assembly causes contact/impact when the distance between the adjacent assemblies becomes less than the initial gap distance.

The displacement responses of both the program developed by us and commercial code (ABAQUS) coincide well with each other. Fig.7 below shows time historical data of contact force for two gap elements. It turned out that the contact/impact timing of gap elements correspond well and the order of the contact force is almost same for both our program and the commercial code. Small difference in the contact force between our program and the commercial code, however, is found in Fig.7. Now we pay attention to the contact criterion, which are used to decide whether a gap element closes or not, to explain this difference. In Fig.7, the contact force of the commercial code occasionally attains negative value. Thus we may consider that the contact criterion of the commercial code allow some tensile force. Conversely our program does not permit the tensile force and only compressive force is caused in fact. Generally speaking it is thought that the tensile force is not generated in the phenomena of the hard contact. That is, this criterion is merely a numerical technique. So it may be considered that the difference between the contact criterion reflects on the difference in the contact force.

4.2   Practical analysis

As a practical analysis we calculate a seismic response of one column (row) core elements of FBR to show an efficiency of our developed program. We show comparisons of deformation of some core elements with a general purpose commercial code (ABAQUS) and estimate the efficiency of the calculation time reduction.

As a model of one column (row) core elements of FBR, four kinds of core element such as fuel assembly (FA), blanket assembly (BA), control rod (CR) and neutron shield (NS) are dealt with. Tab.3 shows the material parameters of these components.

Table 3: Material properties of core elements

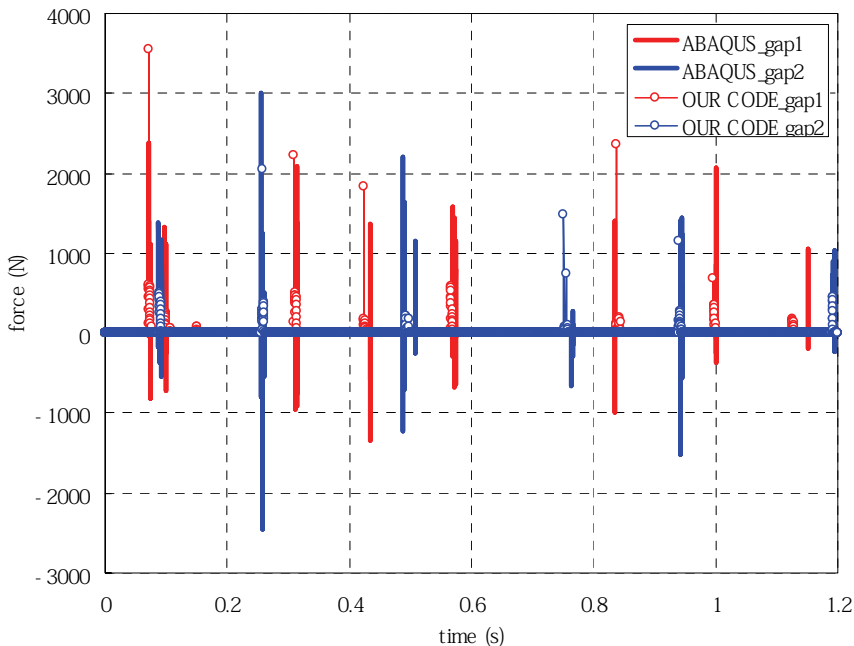|	Young's modulus [Pa]	rigidity [Pa]	Poisson ratio [-]	Rayleigh damping alpha [1/s]	Rayleigh damping beta [s]
FA	1.626e11	6.254e10	0.3	1.003e-1	4.082e-3
BA	1.689e11	6.496e10	0.3	1.009e-1	4.210e-4
CR	1.689e11	6.496e10	0.3	1.407e-1	3.993e-3
NS	1.689e11	6.496e10	0.3	1.555e-1	4.286e-3

Figure 7: Time history of the contact force

One column (row) of core elements consist of 31 core elements such as 16 FAs, 6 BAs, 1 CR and 8 NSs. Walls are located on both sides of the column (row). So in total 33 assembly models are configured as shown in Fig.8 below. (In Fig.8 'W', 'N', 'B', 'F' and 'C' stand for wall, neutron shield, blanket assembly, fuel assembly and control rod respectively.)

The FEM model of assemblies and load pads are shown in Fig. 2. The assembly model consists of 17 beam elements of the body and one spring element of support.(See Tab.4) The load pad consists of the combination elements of spring and dashpot.(See Tab.5) The pads are set on the both sides of the position at the 10th node and the 16th node.

We set boundary conditions for all assemblies as in Fig.9.

In Fig.9, $f(t)$ stands for time historical data of the seismic acceleration as shown in Fig.10. That data is applied to the x-directional translation degree of freedom of support nodes and entrance nozzle nodes. The y-directional and z-directional translation degrees of freedom and all rotation degrees of freedom are fixed at support nodes. A rotation degree of freedom around the y-axis is free at entrance nozzle nodes.
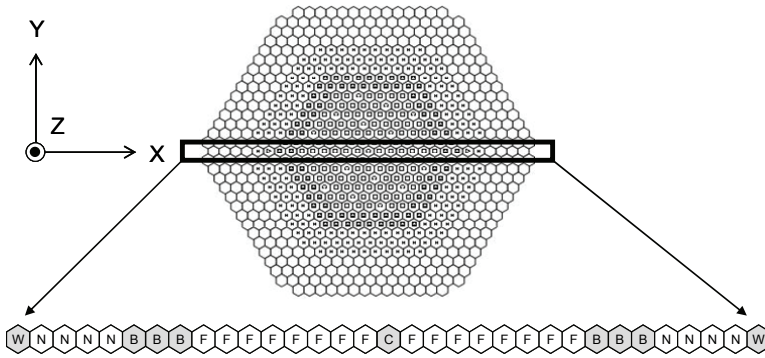
Figure 8: Configuration of the one column (row) of core elements

Table 4: Material properties of the spring of the support

	Spring coefficient [N/m]
FA	5.69e6
BA	3.14e6
CR	8.70e6
NS	5.04e6

Table 5: Material properties of the spring and dashpot of the load pad

		Spring coef. [N/m]	Damping coef. [Ns/m]
FA	Lower pad	4.12e7	1.42e7
	Upper pad	2.75e9	4.24e4
BA	Lowe pad	4.28e8	1.46e4
	Upper pad	2.75e9	4.27e4
CR	Lower pad	2.92e8	3.56e4
	Upper pad	1.96e9	3.16e4
NS	Lower pad	4.28e7	1.58e4
	Upper pad	3.14e9	4.47e4

We show the relative displacement of the top node of the assembly with respect to the support node. Comparisons with the commercial code (ABAQUS) are done for the 16th assembly (CR), the 24th assembly (FA), the 27th assembly (BA) and the 31st assembly (NS).

Very strong nonlinearity appears in this practical example. In fact, at most over 30 gap elements cause contact/impact simultaneously. From these comparisons we can conclude that our proposed algorithm works reasonably well because the re-
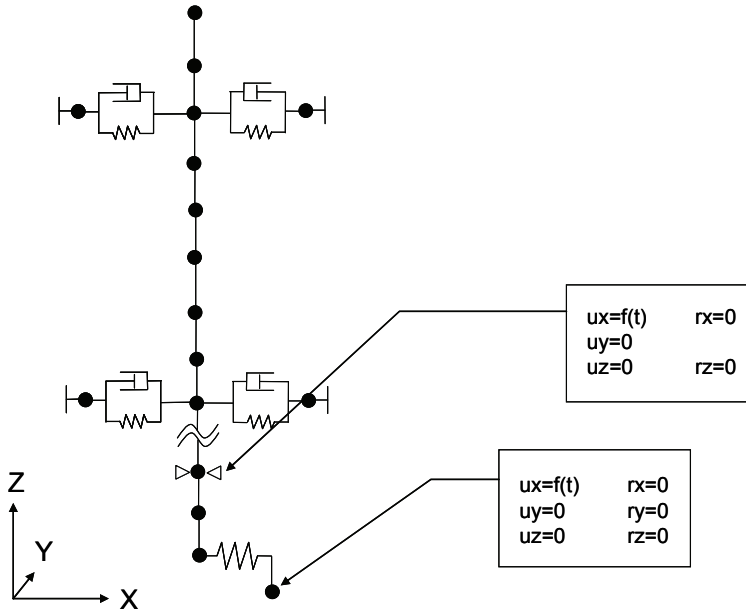
Figure 9: Boundary conditions for an assembly

sults of our developed program coincide well with those of the commercial code (ABAQUS). Next we mention the calculation time of our program and the commercial code (ABAQUS) by using a same PC (Windows Vista, Xeon E5462, 2.80GHz). This practical example deals with a 15 seconds event. The general purpose commercial code (ABAQUS) requires about 4 hours to complete the calculation. On the other hand our program takes about 5 minutes to finish the calculation. Thus we succeeded in decreasing the calculation time by a factor of 40.

4.3   Full model analysis

Finally we carry out the full model analysis of an FBR. We deal with 715 assemblies, in which there are four kinds of core element such as fuel assembly, blanket assembly, control rod and neutron shield. Material properties of them are the same as in Tab.3. We model a rigid wall surrounding all assemblies by rigid assemblies (beam-like structures) located at the outermost positions. So, there are 805 assemblies in total. The assembly model is the same one as in section 4.2. That is, its body, support and load pad consist of 17 beam elements, one spring element and one combination element of spring and dashpot respectively as shown in Tab4. and Tab.5. Fig.15 below shows a configuration of the full model of a whole core. It is
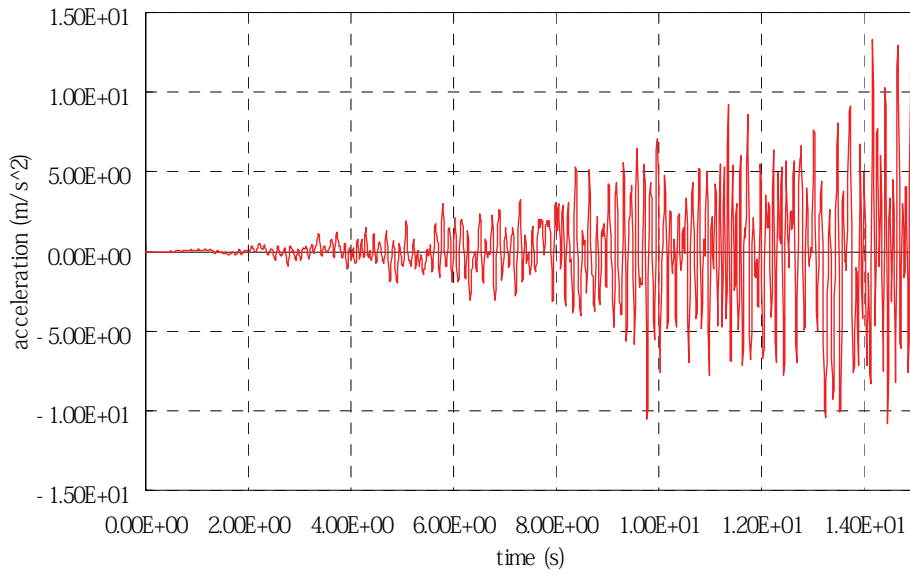
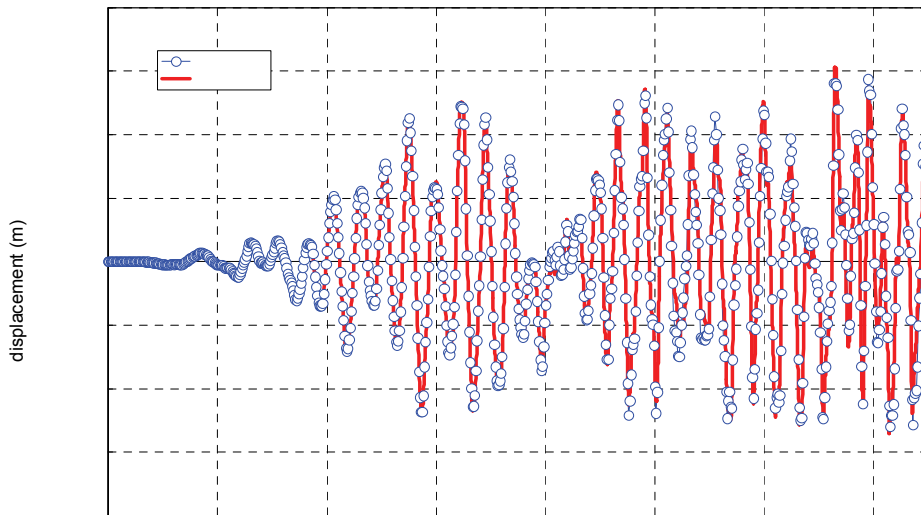Figure 10: Time historical data of the input seismic acceleration

Figure 11: Time history of the relative displacement of the 16th assembly
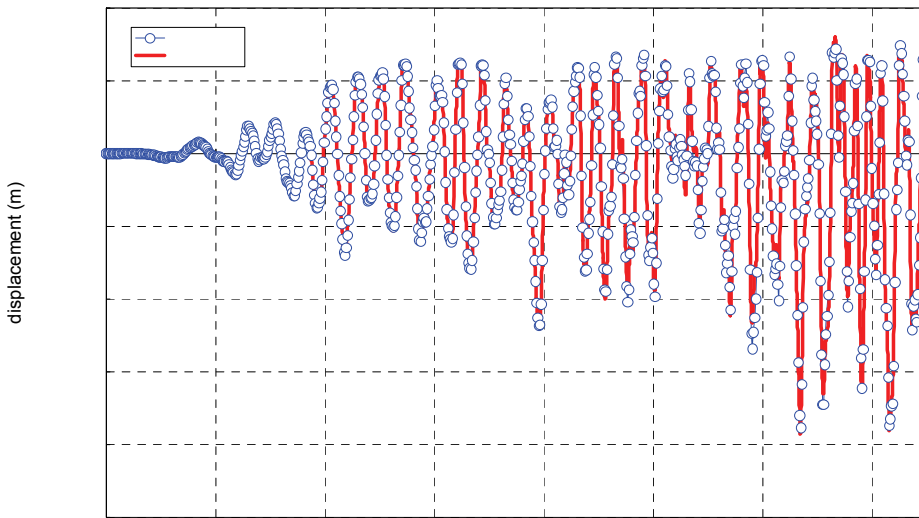
Figure 12: Time history of the relative displacement of the 24th assembly

noted that the configuration of control rods is not symmetric. In Fig.15, the out-ermost structure stands for a rigid wall. Thus the structure is a rigid body and is moved according to a seismic acceleration. Boundary conditions applied to each assembly and input data of a seismic acceleration are the same as in Fig.9 and Fig.10 respectively.

Now we show the relative displacement of the top node of the assembly with re-spect to the support nodes. Comparisons with the commercial code (ABAQUS) are done for the assembly A and the assembly B. (See Fig.15) As shown in Fig.16 and Fig.17, results of our program coincide well with those of the commercial code (ABAQUS).

Next we give some figures, which show the whole core deformation in case the area surrounded by the outer fuel assemblies and the inner fuel assemblies reaches the minimum value.

From Fig.18 and Fig.19 it turns out that all assemblies may be deflected to one direction and cause core compaction due to their contact/impact. Finally we discuss the calculation time of our program and the commercial code (ABAQUS). The calculation time for the full model analysis and the practical analysis shown in section 4.2 are as follows in Tab.6 and Tab.7:

It should be mentioned that it took too much calculation time for ABAQUS to com-
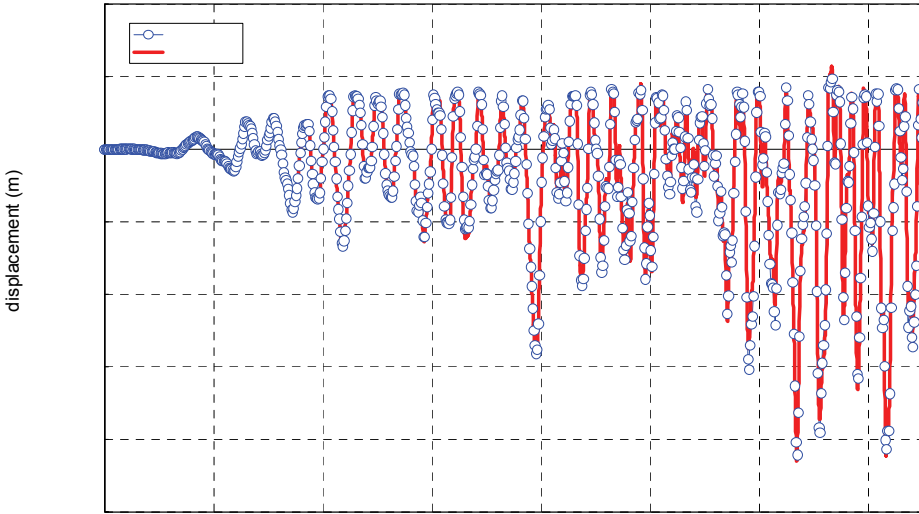
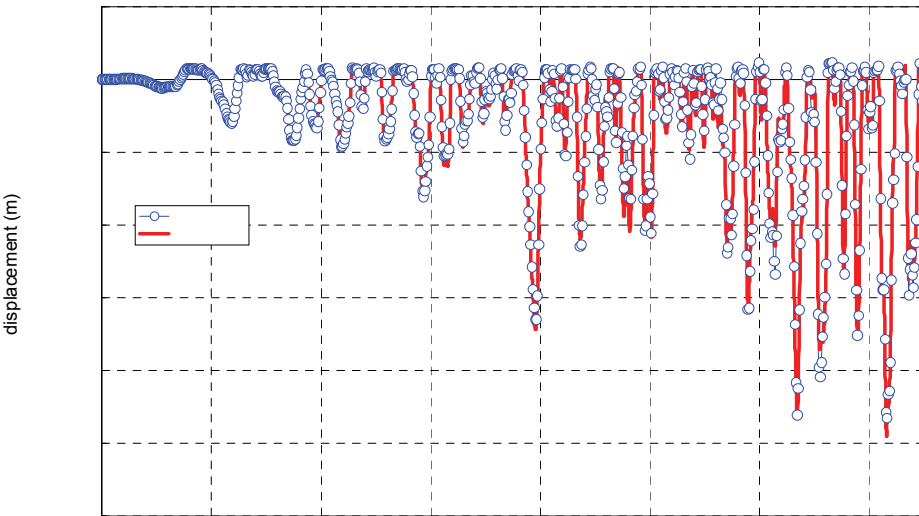Figure 13: Time history of the relative displacement of the 27th assembly

Figure 14: Time history of the relative displacement of the 31st assembly
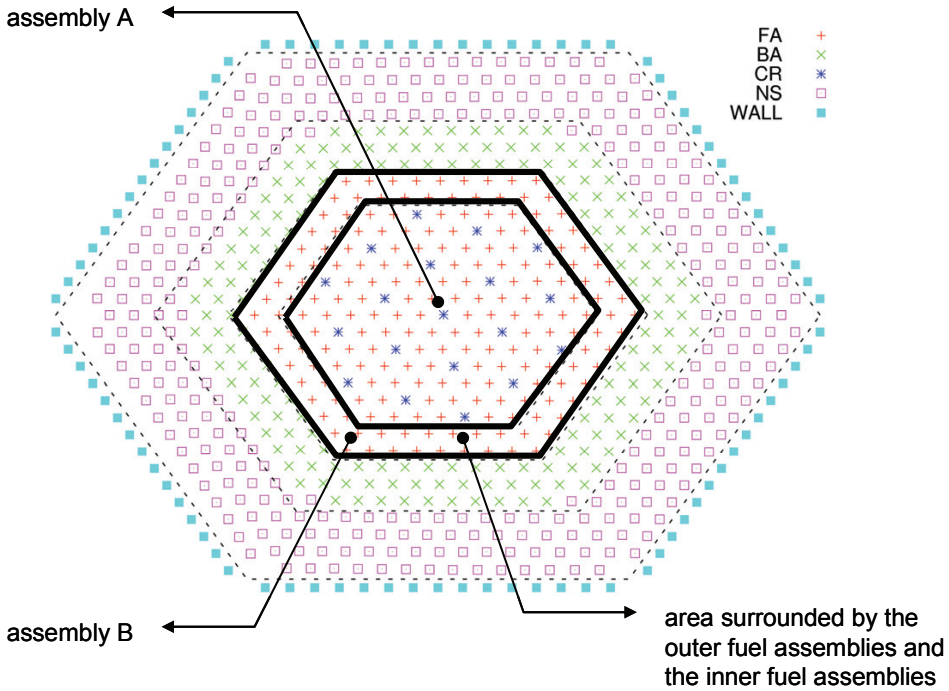
assembly A

FA   +
BA   ×
CR   ✳
NS   ▫
WALL   ■

assembly B

area surrounded by the
outer fuel assemblies and
the inner fuel assemblies

Figure 15: Configuration of the full model of a whole core

Table 6: Comparisons of the calculation time

code	model	seismic event [s]	PC	# of PE	calc. time [hour]
ABAQUS	full model	5	B	6	396
our program	full model	5	A	1	1
our program	full model	15	A	1	5
ABAQUS	small model (one column)	15	C	1	4
our program	small model (one column)	15	C	1	0.083 (=5[min])

(PE stands for "Processor Element".)

Table 7: Specifications of PCs

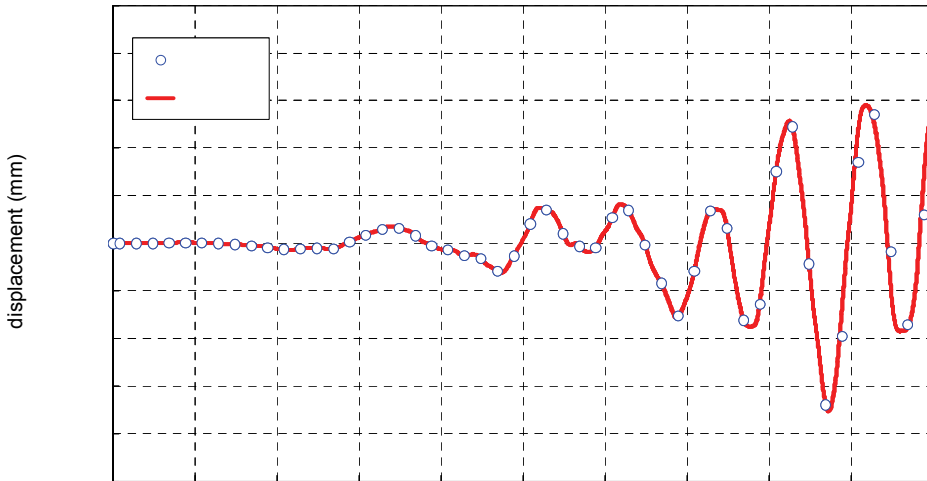| PC	A	B	C
OS	Linux	HITACH SR16000	Windows Vista
CPU	Xeon5570 (2.93GHz)	IBM Power6 (3.5GHz)	XeonE5462 (2.80GHz)
memory	96GB	129GB	32GB

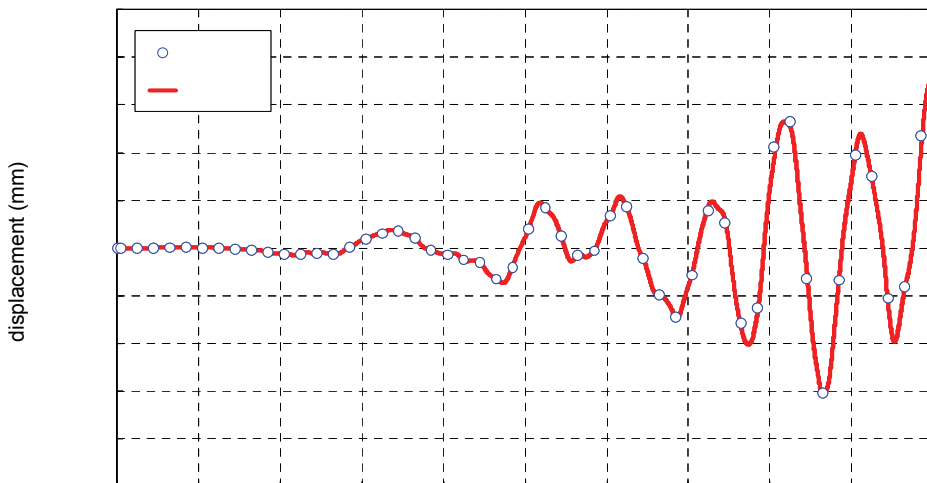Figure 16: Time history of the relative displacement of the assembly A

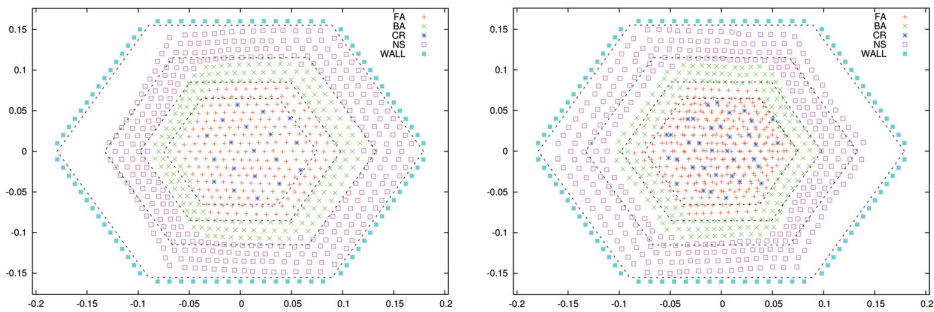Figure 17: Time history of the relative displacement of the assembly B

Figure 18: Cross section view of the whole core deformations (Left figure shows a deformation at 13.32[s] and Right figure shows a deformation at 34.16[s]. Deformation scale factor of these figures is 500%.)
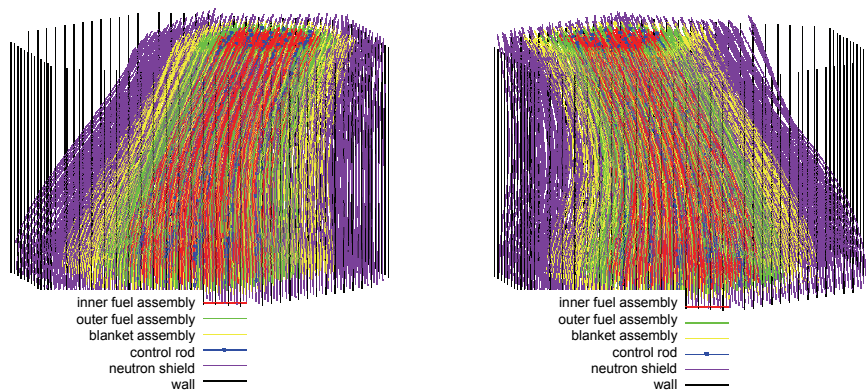

Figure 19: Bird's eye view of the whole core deformations(Left figure shows a deformation at 13.32[s] and Right figure shows a deformation at 34.16[s]. Deformation scale factor of these figures is 500%.)

plete the 15 seconds seismic event reasonably. So, Tab.6 includes only result of the 5 seconds seismic event for ABAQUS. Moreover it should be noted that the memory size of our PC "A" was not enough to finish the calculation for ABAQUS. Then another PC "B" with a similar specification to our PC "A" was used. ABAQUS requires 396 hours to complete the calculation of the 5 seconds event. On the other hand our program takes 5 hours to finish the calculation. We succeeded in decreasing the calculation time by a factor of 400.

5   Conclusion

We proposed a new reduction method for contact problems and developed an FBR core seismic analysis program in terms of the method. Especially we give the details of the formulations and a concrete procedure for implementation. Moreover we show a sufficient condition for the algorithm to work well and a generalization of this method. From three calculation examples it turned out that our method works reasonably well and that using this method succeeds in decreasing the calculation time dramatically. In the future we will apply it for many parameter studies of the full model analysis of FBR core seismic response to design robust FBRs.

References

Geradin, M.; Cardona, A. (2001):*Flexible multibody dynamics: a finite element approach,* John Wiley.

IAEA (1993): Intercomparison of liquid metal fast reactor seismic analysis codes Volume 1: Validation of Seismic Analysis Codes using Reactor Core Experiments (*IAEA-TECDOC-798*), Vienna (Austria), 16-17 Nov., 1993.

IAEA (1994): Intercomparison of liquid metal fast reactor seismic analysis codes Volume 2: Verification and Analysis Codes using Core Mock-up Experiments (*IAEA-TECDOC-829*), Vienna (Austria), 26-28 Sep., 1994.

IAEA (1995): Intercomparison of liquid metal fast reactor seismic analysis codes Volume 3: Comparison of observed effects with computer simulated effects on reactor cores from seismic disturbances (*IAEA-TECDOC-882*), Bologna (Italy), 30 May-2 June, 1995.

Kobayashi,T. (1995): Evaluation of LMFBR core seismic analysis by the SAL-CON code, intercomparison of liquid metal fast reactor seismic analysis codes Volume 3: Comparison of observed effects with computer simulated disturbances (*IAEA-TECDOC-882*), 113-149, Bologna (Italy), 30 May-2 June, 1995.

Nakagawa, M. (1986): ARKAS: A three-dimensional finite element program for core-wide mechanical analysis of liquid-metal fast breeder reactor cores *Nucl. Technol.*, Vol.75, pp.46-45.